

# Structural Control of the Reversible Dimerization of $\pi$ -Conjugated Oligomeric Cation Radicals

Eric Levillain and Jean Roncali\*

Contribution from the Ingénierie Moléculaire et Matériaux Organiques, CNRS UMR 6501, Université d'Angers, 2 Bd Lavoisier, 49045 Angers, France

Received March 9, 1999

**Abstract:** The reversible dimerization of the electrochemically or chemically generated cation radicals of diversely substituted tetrathienylenevinylens (**1–6**) has been analyzed by concentration and temperature-dependent cyclic voltammetry, UV–vis, near-IR, and ESR spectroscopies, and time-resolved spectroelectrochemistry. For unsubstituted and end-substituted oligomers **1** and **2** the apparent redox potential corresponding to the formation of the cation radical (E<sub>app1</sub>) shifts negatively when increasing substrate concentration or when decreasing temperature, as expected for an EC<sub>Dim</sub>E scheme. Such effects are not observed for compounds **3–6** containing  $\beta$ -substituted thiophene rings suggesting that the corresponding cation radicals do not dimerize. UV–vis and near-IR absorption spectra of the chemically generated cation radical **2**<sup>•+</sup> show, in addition to the two absorption bands of the monomeric cation radical, two hypsochromically shifted transitions confirming that **2**<sup>•+</sup> dimerizes already at room temperature. These additional spectral features are not observed for **6**<sup>•+</sup> even at low temperature. These quite different behaviors are confirmed by temperature-dependent ESR experiments which show that whereas the ESR signature of **2**<sup>•+</sup> vanishes at low temperature, that of **6**<sup>•+</sup> persists even in the frozen state at 150 K. These various sets of results thus provide conclusive evidences for a structural control of the reversible dimerization of oligomeric cation radicals.

## Introduction

For about 15 years, the process of charge transport in doped conjugated polymers with a nondegenerate ground state such as polythiophene has been essentially discussed in the frame of the polaron/bipolaron paradigm.<sup>1</sup> The considerable intensification of research on monodisperse  $\pi$ -conjugated oligomers during the past decade has greatly contributed to improve the level of understanding of the electronic and electrochemical properties of the parent polydisperse polymers. In particular a large amount of work has been focused on the analysis of the chain length dependence of these relevant properties, while extrapolations of the data obtained on short-chain oligomers have been widely used in order to predict the ultimate electronic and electrochemical properties of an ideal defect-free polymer chain.<sup>2</sup> As an unexpected consequence of these studies, the discovery of the reversible dimerization of oligothiophenes (nTs) cation radicals and the proposal of diamagnetic interchain  $\pi$ -dimers as alternative to bipolarons in the interchain charge-transport of doped conjugated polymers has exerted a profound influence on the general perception of the mechanisms of charge transport in conducting polymers.<sup>3–9</sup> Since the initial report of Miller et al. on the cation radicals of short chain nTs,<sup>3a</sup> the dimerization of cation radicals has been observed on a great variety of

$\pi$ -conjugated structures including extended nTs,<sup>4</sup> nTs substituted by alkyl, phenyl, carboxylic acid, methoxy, or phenyldimethylsilyl groups,<sup>5</sup> end-capped oligopyrroles,<sup>6</sup> oligophenylenevinylens,<sup>7</sup> and mixed oligomeric systems involving phenyl, thiophene or pyrrole rings.<sup>8</sup>

Although to date all reports of intermolecular reactions between radical cations of conjugated systems postulate the formation of  $\pi$ -dimers, Heinze et al. have recently reported evidences for the reversible formation of  $\sigma$ -dimers between cation radicals of diphenylpolyenes, 3,3',5,5'-tetramethylbithiophene, and phenylenevinylens.<sup>9</sup>

On the basis of these various studies, it has been suggested that dimerization is a rather universal property of conjugated

(1) (a) T. C. Chung, T. C.; Kaufman, J. H.; Heeger, A. J.; Wudl, F. *Phys. Rev.* **1984**, *B30*, 702. (b) Heeger, A. J.; Kivelson, S.; Schrieffer, J. R.; Su, W.-P. *Rev. Mod. Phys.* **1988**, *781*, 60. (c) Brédas, J. L.; Thémans, B.; André, J. M.; Chance, R. R.; Silbey, R. *Synth. Met.* **1984**, *9*, 265.

(2) (a) Heinze, J.; Mortensen, J.; Müllen, K.; Schenk, R. *J. Chem. Soc. Chem. Commun.* **1987**, 701. (b) Caspar, J. V.; Ramamurthy, V.; Corbin, D. R. *J. Am. Chem. Soc.* **1991**, *113*, 600. (c) Bäuerle, P. *Adv. Mater.* **1992**, *4*, 102. (d) Guay, J.; Kasai, P.; Diaz, A.; Wu, R.; Tour, J. M.; Dao, L. H. *Chem. Mater.* **1992**, *4*, 1097. (e) Havinga, E. E.; Meijer, E. W.; ten Hoeve, W.; Wynberg, H. *Synth. Met.* **1991**, *41–43*, 473. (f) Bäuerle, P.; Segelbacher, U.; Gaudl, K. U.; Huttenlocher, M.; Mehring, M. *Angew. Chem., Int. Ed. Engl.* **1993**, *32*, 76.

(3) (a) Hill, M. G.; Mann, K. R.; Miller, L. L.; Penneau, J. F. *J. Am. Chem. Soc.* **1992**, *114*, 2728. (b) Hill, M. G.; Mann, K. R.; Miller, L. L.; Penneau, J. F.; Zinger, B. *Chem. Mater.* **1992**, *4*, 1106. (c) Bäuerle, P.; Segelbacher, U.; Maier, A.; Mehring, M. *J. Am. Chem. Soc.* **1993**, *115*, 10217.

(4) (a) Bäuerle, P.; Fisher, T.; Bidlingmeier, B.; Stabel, A.; Rabe, J. *Angew. Chem., Int. Ed. Engl.* **1995**, *34*, 303. (b) van Haare, J. A. E. H.; Havinga, E. E.; van Dongen, J. L. J.; Janssen, R. A. J.; Cornil, J.; Brédas, J.-L. *Chem. Eur. J.* **1998**, *4*, 1509.

(5) (a) Miller, L. L.; Yu, Y.; Gunic, E.; Duan, R. *Adv. Mater.* **1995**, *7*, 547. (b) Hong, Y.; Yu, Y.; Miller, L. L. *Synth. Met.* **1995**, *74*, 133. (c) Yu, Y.; Gunic, E.; Zinger, B.; Miller, L. L. *J. Am. Chem. Soc.* **1996**, *118*, 1013. (d) Graf, D. D.; Duan, R. G.; Campbell, J. P.; Miller, L. L.; Mann, K. R. *J. Am. Chem. Soc.* **1997**, *119*, 5888.

(6) van Haare, J. A. E. H.; Gronendaal, L.; Havinga, E. E.; Janssen, R. A.; Meijer, E. W. *Angew. Chem., Int. Ed. Engl.* **1996**, *35*, 638.

(7) Sakamoto, A.; Furukawa, Y.; Tasumi, M. *J. Phys. Chem. B* **1997**, *101*, 1726.

(8) (a) van Haare, J. A. E. H.; van Bostel, M.; Janssen, R. A. J. *Chem. Mater.* **1998**, *10*, 1166. (b) van Haare, J. A. E. H.; Gronendaal, L.; Havinga, E. E.; Meijer, E. W.; Janssen, R. A. *Synth. Met.* **1997**, *85*, 1091.

(9) (a) Smie, A.; Heinze, J. *Angew. Chem., Int. Ed. Engl.* **1997**, *36*, 363. (b) Tschuncky, P.; Heinze, J.; Smie, A.; Engelmann, G.; Kossmehl, G. *J. Electroanal. Chem.* **1997**, *433*, 223. (c) Heinze, J.; Tschuncky, P.; Smie, A. *J. Solid State Electrochem.* **1998**, *2*, 102.

oligomeric cations and that steric factors have no significant effect on dimerization.<sup>3c,10</sup>

However, one may wonder whether steric burial of the  $\pi$ -conjugated system by introduction of bulky substituents may be capable to impose intermolecular distances large enough to inhibit the dimerization process.

We have recently synthesized various series of oligothiophenevinylenes (nTVs) as a new class of extensively  $\pi$ -conjugated linear systems and reported some first investigations of the chain length dependence of their electronic and electrochemical properties.<sup>11</sup> More recently, the analysis of the electrochemical and optical properties of nTVs end-capped with dithiafulvenyl groups led to conclusive evidence for reinforced intermolecular interactions due to the well-known propensity of dithiafulvenyl groups to self-assemble into regular  $\pi$ -stacks.<sup>12</sup> On the other hand, a preliminary electrochemical analysis of nTVs end-capped with Fréchet-type dendritic branches of increasing generation number showed unambiguously that the first redox potential of the nTV electrophore was quite independent of scan rate and substrate concentration, thus suggesting that the corresponding cation radical is not subject to a follow-up chemical reaction.<sup>13</sup>

These first indications for a structural modulation of the interchain interactions in nTVs provided a strong incitement to undertake more systematic investigations of the relationships between the molecular structure of nTVs and the ability of the corresponding cation radicals to undergo reversible dimerization.

As a first step in this direction, we report here an analysis of the electrochemical and optical properties of the electrochemically and chemically generated cation radicals derived from diversely substituted nTVs. To this end, oligomer chain length was deliberately limited to the tetramer (4TV) because of the direct formation of the dication occurring for longer chains.<sup>11</sup> Using the unsubstituted compound (**1**) as basic structure, two, four, and six alkyl substituents were progressively introduced at various positions of the 4TV structure (compounds **2–6**) (for structures, see Scheme 1). Chemically or electrochemically generated cations radicals of these various compounds have been characterized in detail by cyclic voltammetry, UV-vis and ESR spectroscopies, and time-resolved spectroelectrochemistry. All of the results of these various experiments provide unequivocal evidences for a structural control of the process of reversible dimerization of nTVs cation radicals.

## Results and Discussion

At ambient temperature, the cyclic voltammogram of compounds **1–6** in methylene chloride exhibits two reversible one-electron oxidation processes corresponding to the successive generation of the cation radical and dication at apparent redox potentials  $E_{app1}$  and  $E_{app2}$  (Table 1). The differences in the values of  $E_{app1}$  and  $E_{app2}$  observed among the various 4TVs are related to the +I effect of alkyl chains which induces a negative shift of  $E_{app1}$  and  $E_{app2}$  from **1** to **6** as the number of alkyl substituents increases.

As shown in Figure 1, a plot of  $E_{app1}$  versus initial substrate concentration ( $C_0$ ) reveals two different behaviors. For com-

**Table 1.** Cyclic Voltammetric Data for Compounds **1–6**<sup>a</sup>

compd	$E_{app1}$ (V)	$E_{app2}$ (V)	$\delta E_{app1}/\delta \log C_0$ (mV)	$\delta E_{app2}/\delta \log C_0$ (mV)
<b>1</b>	0.751		-29	
<b>2</b>	0.684	0.895	-29	+29
<b>3</b>	0.680	0.865	0	0
<b>4</b>	0.642	0.882	0	0
<b>5</b>	0.574	0.780	0	0
<b>6</b>	0.573	0.782	0	0

<sup>a</sup>  $c = 2 \times 10^{-3}$  mol L<sup>-1</sup> in  $2 \times 10^{-1}$  mol L<sup>-1</sup> TBAHP/CH<sub>2</sub>Cl<sub>2</sub>; Pt electrodes, ref Ag·AgCl, scan rate 100 mV s<sup>-1</sup>.

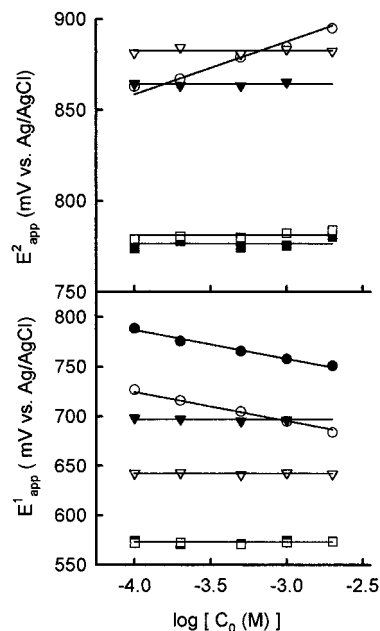


**Figure 1.** Plots of  $E_{app1}$  (determined in the conditions of Table 1) vs substrate concentration ( $C_0$ ) for compounds **1–6**: **1** (●), **2** (○), **3** (▼), **4** (▽), **5** (■), **6** (□) (ref Ag·AgCl).

pounds **3–6** which contain thiophenes substituted at the 3 or 3 and 4 positions,  $E_{app1}$  is quite independent of  $C_0$ . In contrast for compounds **1** and **2**,  $E_{app1}$  decreases linearly with  $\log(C_0)$  with a slope of  $-29$  mV/log unit. Such a variation, already observed for oligothiophenes,<sup>14</sup> is characteristic for a mechanism involving the reversible dimerization of two radical cations according to an  $EC_{Dim}E$  scheme.<sup>15</sup> The variation of  $E_{app1}$  with  $C_0$  and the equilibrium constant  $K$  are given by

$$KC_0 \gg 1, E_{app1} = E^{\circ 1} - RT/2F \log(KC_0) - 0.22RT/2F \quad (1)$$

$$KC_0 \ll 1, E_{app1} = E^{\circ 1} \quad (2)$$

where  $E^{\circ 1}$  is the normal potential of the 4TV<sup>•+</sup>/4TV couple under consideration.

In our case, the invariance of  $E_{app1}$  with scan rate ( $\nu$ ) between 0.10 and 100 V s<sup>-1</sup>, indicates that the dimerization equilibrium is fast. The peak currents scale linearly with  $\nu^{1/2}$ , as expected for a diffusion-controlled process.

In the case of diphenylpolyenes and tetramethyl 3,3',5,5'-tetramethylbithiophene, it has been reported that increasing scan rate or decreasing temperature led to the appearance of a new

(10) Miller, L. L.; Mann, K. R. *Acc. Chem. Res.* **1996**, *29*, 417.

(11) (a) Elandaloussi, E.; Frère, P.; Roncali, J. *Chem. Commun.* **1997**, 301. (b) Elandaloussi, E.; Frère, P.; Richomme, P.; Orduña, J.; Garin, J.; Roncali, J. *J. Am. Chem. Soc.* **1997**, *119*, 10774. (c) Jestin, I.; Frère, P.; Blanchard, P.; Roncali, J. *Angew. Chem., Int. Ed. Engl.* **1998**, *37*, 942. (d) Jestin, I.; Frère, P.; Mercier, N.; Levillain, E.; Stievenard, D.; Roncali, J. *J. Am. Chem. Soc.* **1998**, *120*, 8150.

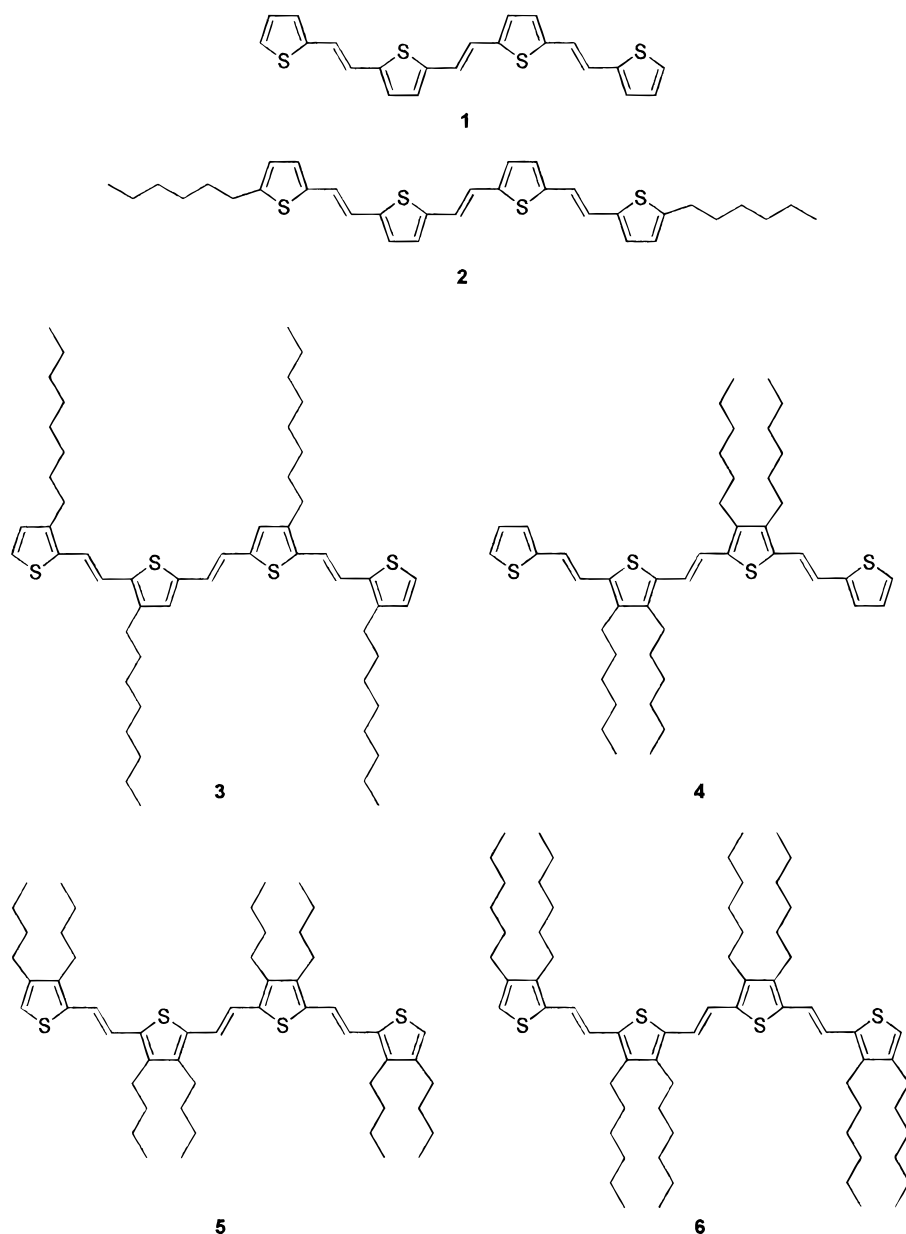
(12) Jestin, I.; Frère, P.; Levillain, E.; Roncali, J. *Adv. Mater.* **1999**, *11*, 134.

(13) Jestin, I.; Levillain, E.; Roncali, J. *Chem. Commun.* **1998**, 2655.

(14) (a) Audebert, P.; Hapiot, P.; Pernaut, J. M.; Garcia, P. *J. Electroanal. Chem.* **1993**, *361*, 283. (b) Hapiot, P.; Audebert, P.; Monnier, K.; Pernaut, J. M.; Garcia, P. *Chem. Mater.* **1994**, *6*, 1549.

(15) (a) Savéant, J. M.; Vianello, E. *Electrochim. Acta* **1967**, *12*, 1545. (b) C. Amatore, C.; Garreau, G.; Hammi, M.; Pinson, J.; Savéant, J. M. *J. Electroanal. Chem.* **1985**, *184*, 1.

## Scheme 1



cathodic wave, at 0.0–0.1 V vs Ag•AgCl, attributed to the reduction of the  $\sigma$ -dimer.<sup>9a,b</sup>

In our case such a wave was never observed when varying the scan rate between 0.10 and 100 V s<sup>-1</sup> and the temperature between 310 and 220 K. The lack of observation of such a wave seems more in favor of the formation of  $\pi$ -dimers, although a definitive conclusion cannot be drawn at this stage of the work.

As appears in Table 1, whereas E<sub>app2</sub> is concentration independent for compounds 3–6, for 2 a linear dependence versus log(C<sub>0</sub>) with a slope of +29 mV/decade opposite to that of E<sub>app1</sub> is observed, as theoretically expected.<sup>16</sup> However, for compound 1 no reliable data could be obtained concerning the concentration dependence of E<sub>app2</sub> because of the precipitation consecutive to the first oxidation step.

A quantitative analysis of the data over the whole concentration range investigated was carried out with the aid of digital simulation.<sup>17</sup> Using one set of simulation parameters,<sup>18</sup> the fit involves concentration changes over one decade. Excellent

agreement between experiment and simulation is found, giving an equilibrium constant of  $K = 1 \times 10^5 \text{ mol}^{-1} \text{ L}$ , (according to eq 1,  $K \gg 1 \times 10^4 \text{ mol}^{-1} \text{ L}$ ) and a forward reaction constant  $k_f$  of  $1 \times 10^9 \text{ mol}^{-1} \text{ s}^{-1}$  (based on the kinetic zone (DE) of the diagrams in ref 15b,  $k_f$  must be greater than  $1 \times 10^9 \text{ mol}^{-1} \text{ s}^{-1}$ ). In these conditions, simulation confirms a +29 mV slope per concentration decade for the second oxidation potential at 293 K.

The variation of E<sub>app1</sub> versus temperature (*T*) has been investigated in the 220 K < *T* < 310 K range for a concentration of substrate of  $2 \times 10^{-3} \text{ mol L}^{-1}$ . For compounds 1 and 2 plots of E<sub>app1</sub> versus *T* give straight lines with slopes of 0.37 and 0.99 mV K<sup>-1</sup>, respectively. The absence of slope inflection up to 310 K indicates that the investigated temperature range corresponds to the predominance of the dimer while that of the cation radical lies beyond the highest accessible temperature in CH<sub>2</sub>Cl<sub>2</sub>. Although this result does not allow the determination

(16) Meunier-Prest, R.; Laviron, E. *J. Electroanal. Chem.* **1996**, *184*, 1.  
 (17) Digisim 2.1.

(18) Charge-transfer parameters  $k_s = 1 \times 10^{-2} \text{ cm s}^{-1}$ ,  $\alpha = 0.5$ . Chemical reaction parameters:  $K = 1 \times 10^5 \text{ mol}^{-1}$ ,  $k_f = 1 \times 10^{10} \text{ mol}^{-1} \text{ s}^{-1}$ ,  $D = 1.8 \times 10^{-6} \text{ cm}^2 \text{ s}^{-1}$ .

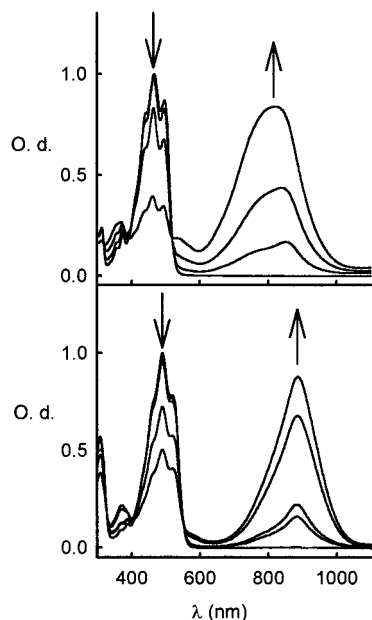


**Figure 2.** UV-vis absorption spectra corresponding to the generation of the cation radical by addition of  $\text{CF}_3\text{COOH}$  to  $2.5 \times 10^{-4} \text{ mol L}^{-1}$  solutions of compound **2** (top) and **6** (bottom) in  $\text{CH}_2\text{Cl}_2$ .

of the equilibrium constant  $K$ , according to eq 1, a value larger than  $1 \times 10^4 \text{ mol}^{-1}$  can be assumed.

No temperature dependence of  $E_{\text{app}1}$  was observed for compounds **3–6**. This suggests, in agreement with the absence of concentration effect, that the cation radicals of these compounds are considerably less prone to dimerize than those of compounds **1** and **2**. This quite different behavior implies that if nevertheless dimerization occurs for compounds **3–6**, the equilibrium constant must be much smaller than  $5 \times 10^2 \text{ mol}^{-1}$  (eq 2).

To go into more detail, the optical properties of the cation radicals of compounds **2** and **6** ( $2^{+\bullet}$  and  $6^{+\bullet}$ ), taken as representative examples of the two classes of compounds, have been investigated by UV-vis and near-IR spectroscopies. Figure 2 shows the evolution of the electronic absorption spectra corresponding to the chemical generation of  $2^{+\bullet}$  and  $6^{+\bullet}$  by addition of increasing amounts of  $\text{CF}_3\text{COOH}$  to methylene chloride solutions. The spectrum of neutral **6** shows a first transition at 320 nm followed by a broader absorption band with a well resolved vibronic fine structure. The absorption maximum is observed at 489 nm while that of the transition of lowest energy ( $\lambda_{0-0}$ ) occurs at 542 nm. Oxidation into  $6^{+\bullet}$  leads to the decrease of the intensity of these bands with the emergence of a weak band at 360 nm (3.44 eV) and of a well-shaped symmetrical band at 880 nm (1.40 eV). This latter transition corresponds to the first subgap transition of the polaron state while the 360 nm band can be assigned to the extra gap third transition theoretically predicted for a positive polaron.<sup>19</sup>

In the neutral state the spectrum of compound **2** is rather similar to that of compound **6** with however an hypsochromic shift of  $\lambda_{\text{max}}$  and  $\lambda_{0-0}$  to 465 and 528 nm, respectively. These blue shifts reflect a decrease of the overall electronic releasing effect due to the smaller number of alkyl substituents. On the other hand, the spectrum of  $2^{+\bullet}$  differs markedly from that of  $6^{+\bullet}$  and shows, in addition to the main band at 860 nm (1.44 eV), the emergence of a new band at 750 nm (1.65 eV).

Figure 3 shows the UV-vis and near-IR spectra of  $2^{+\bullet}$  and  $6^{+\bullet}$  generated by addition of increasing amounts of the neutral

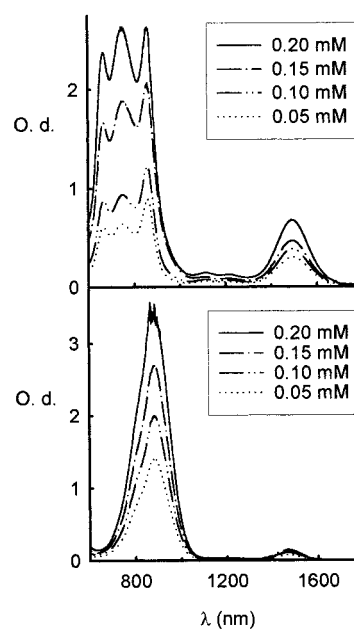


**Figure 3.** UV-vis and near-IR absorption spectra corresponding to the generation of  $2^{+\bullet}$  (top) and  $6^{+\bullet}$  (bottom) for various concentrations of substrate to a solution of  $\text{CF}_3\text{COOH}$  (50% in methylene chloride).

compounds in a methylene chloride solution of trifluoroacetic acid. This procedure allows an analysis of the concentration effect while ensuring a maximal oxidation to the cation radical state in the whole concentration range investigated. In addition to the already discussed main band at 880 nm, the spectrum of  $6^{+\bullet}$  shows a band of weak intensity at 1500 nm (0.82 eV) corresponding to the subgap transition of lowest energy of the cation radical. While these two transitions are also present in the spectrum of  $2^{+\bullet}$  at 860 and 1480 nm (1.44 and 0.84 eV), this spectrum shows several additional features namely a band of weak intensity at 1120 nm (1.12 eV) and two intense bands at 670 and 750 nm (1.85 and 1.65 eV). By analogy with previous works on oligomeric cation radicals,<sup>3–9</sup> the new bands at 1.12 and 1.85 eV can be assigned to the dimers of the cation radical while the band at 1.65 eV can be attributed to a vibronic replica of the band at 1.85 eV. The Davydov energy shift between the transitions of the monomeric and dimeric cation ( $\sim 0.20 \text{ eV}$ ) are smaller than those reported for oligothiophenes<sup>3–5</sup> and tetrathiafulvalenes.<sup>20</sup> However, since it has been observed that the energy splitting gradually decreases with the conjugation length,<sup>3c</sup> this difference can be attributed to the larger effective conjugation length of nTVs. Further examination of the spectra in Figure 3 shows that the intensity of the dimer band at 750 nm relative to that of the monomeric cation radical at 860 nm increases when the concentration of substrate and hence of cation radical increases. This behavior is consistent with a higher equilibrium concentration of the dimer at higher concentration of the substrate.<sup>3a,5c</sup> This effect becomes particularly evident in Figure 4 which shows that a further increase in substrate concentration leads to a considerable intensification of the spectral signature of the dimer. Furthermore, the presence of an absorption tail in the low-energy side of the spectrum suggests that it might contain the weak charge-transfer band of the dimer which is generally observed in this spectral region.<sup>3c,5c</sup>

These results confirm, in agreement with electrochemical data, that  $2^{+\bullet}$  undergoes considerable dimerization already at room temperature which is not the case for  $6^{+\bullet}$ . To check the

(19) Cornil, J.; Beljonne, D.; Brédas, J. L. *J. Chem. Phys.* **1995**, *103*, 834.

(20) Torrance, J. B.; Scott, B. A.; Welber, B.; Kaufman, F. B.; Seiden, P. E. *Phys. Rev. B* **1979**, *19*, 730.

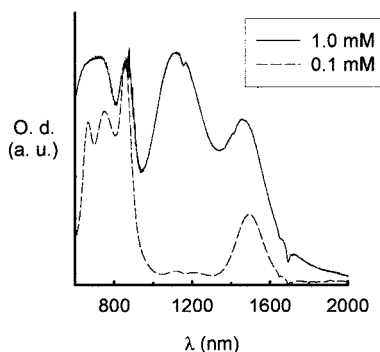


**Figure 4.** Normalized optical spectra UV-vis and near-IR absorption spectra corresponding to the generation of  $2^{+}$  in the conditions of Figure 3.

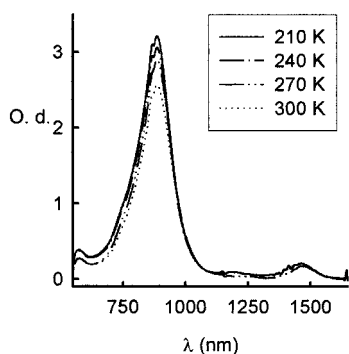


**Figure 5.** Temperature-dependent UV-vis and near-IR spectra of the  $6^{+}$  (0.20 mM) chemically generated in the conditions of Figure 4.

possibility that dimerization of this latter species takes place at a lower temperature, the optical spectrum of  $6^{+}$  has been recorded in the 300–210 K range. As shown in Figure 5, except for minor changes in intensity due to solvent contraction, decreasing the temperature down to 210 K has practically no effect on the spectrum, which agrees well with an absence of dimerization.

Definitive confirmation of this conclusion is given by the comparison of the temperature-dependent ESR spectra of electrogenerated  $2^{+}$  and  $6^{+}$  (Figure 6). The ESR line shape of  $2^{+}$  can be adjusted to a Lorentzian signal, with  $g = 2.0009 \pm 0.0001$  and  $\Delta H_{pp}$  close to  $6.0 \pm 0.2$  G at 300 K. When the temperature is decreased, the ESR signal progressively vanishes with almost complete extinction at 260 K. These results lead to an estimated enthalpy of dimerization of  $\sim 48$  kJ mol $^{-1}$ . While this result is comparable to those reported for oligothiophenes,<sup>3,4</sup> such high values have been considered as an argument for  $\sigma$ -dimer formation.<sup>9</sup> For  $6^{+}$  the ESR line shape can be adjusted to a Lorentzian signal, with  $g = 1.9992 \pm 0.0001$  and  $\Delta H_{pp}$  close to  $3.70 \pm 0.02$  G at 300 K. However, contrary to  $2^{+}$ , the decrease of the temperature produces an intensification of the ESR signal in agreement with Curie's law, and the paramagnetic signal assigned to the monomeric cation radical is still observed even in the frozen state (150 K).

To obtain a global illustration of these quite different behaviors, the electrooxidation of compounds **2** and **6** has been analyzed by time-resolved UV-vis and near-IR spectroelectrochemistry in thin-layer conditions. Figures 7 and 8 show the evolution of the optical spectrum of the two compounds during a forward potential scan at low scan rate. The lower  $E_{app1}$  and  $E_{app2}$  values for compound **6** are reflected by the less positive potential needed to observe the onset of the characteristic spectral features of the cation radical and dication. On the other hand, the spectroelectrochemical curves for compound **2** clearly

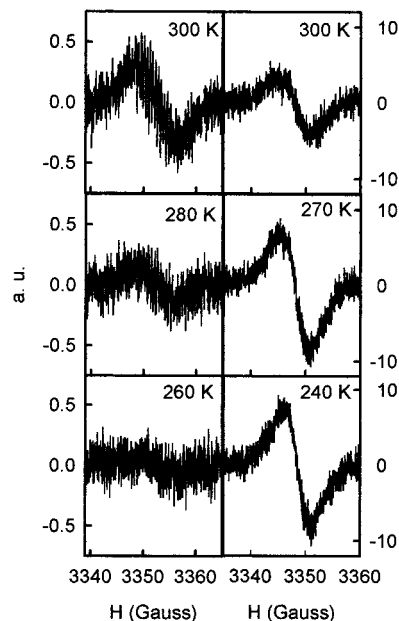


**Figure 6.** Temperature-dependent ESR spectra of in-situ-electrogenerated  $2^{+}$  (left) and  $6^{+}$  (right)  $10^{-3}$  mol L $^{-1}$  in  $2 \times 10^{-1}$  mol L $^{-1}$  TBAHP/CH $_2$ Cl $_2$ .

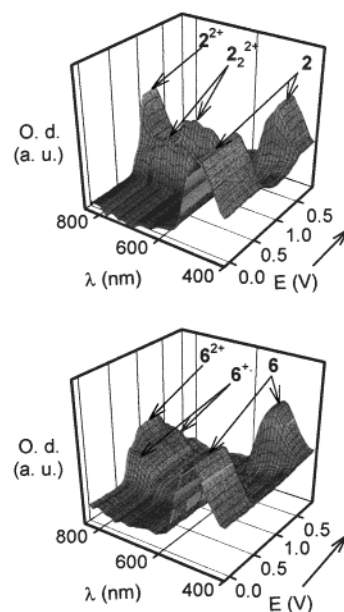


**Figure 7.** Time-resolved UV-vis spectroelectrochemistry in thin layer conditions. ( $d \approx 50$   $\mu$ m):  $c = 10^{-3}$  mol L $^{-1}$  in  $4 \times 10^{-1}$  mol L $^{-1}$  TBAHP/CH $_2$ Cl $_2$ . Spectra recorded during a complete voltammetric cycle at 0.1 mV s $^{-1}$ . Top (**2**), bottom (**6**) (ref Ag $\cdot$ AgCl).

show the development of the characteristic spectral features of the  $\pi$ -dimers in both the visible (600–750 nm) and near-IR (1000–1250 nm) regions when the potential reaches the first anodic peak.

## Conclusion

The electrochemical and optical properties of the cation radicals of a series of diversely substituted 4TVs have been analyzed. Whereas the cation radical of unsubstituted or end-substituted oligomers readily dimerize already at room temperature, similarly to oligothiophenes, substitution at the  $\beta$ -positions of the thiophene rings inhibits the dimerization process in striking contrast with oligothiophenes. Although we have at

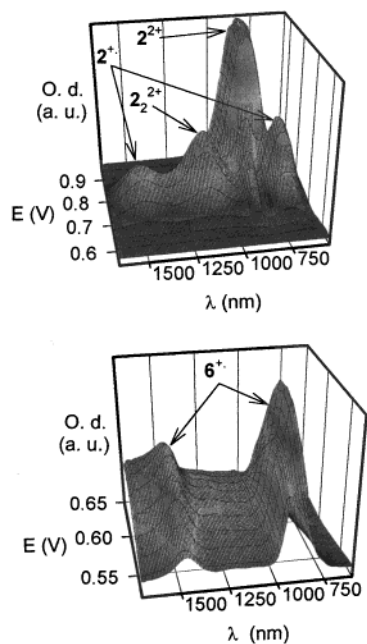


**Figure 8.** Time-resolved near-IR spectroelectrochemistry in thin layer conditions. ( $d \approx 50 \mu\text{m}$ ):  $c = 10^{-3} \text{ mol L}^{-1}$  in  $4 \times 10^{-1} \text{ mol L}^{-1}$  TBAHP/ $\text{CH}_2\text{Cl}_2$ . Scan rate  $0.1 \text{ mV s}^{-1}$ . Top (2), bottom (6) (ref Ag/AgCl).

present no definitive explanation for this astonishing result, several factors may be invoked such as the more restricted conformational flexibility of nTVs, a different distribution of the positive charge over the whole conjugated oligomeric molecule, or the lower sulfur content of nTVs, since  $\text{S}\cdots\text{S}$  interactions can constitute a driving force for cation radical dimerization, as widely demonstrated for the cation radical salts of tetrathiafulvalene derivatives.<sup>21</sup>

From a technical viewpoint, these results can already have important consequences for applications of linear  $\pi$ -conjugated systems as active materials where the strengthening or in contrast the weakening of intermolecular interactions plays a determining role such organic field effects transistors<sup>22</sup> or light-emitting diodes.<sup>23</sup> At a more basic level they also underline the need for further investigations to achieve a better understanding of the

(21) Williams, J. M.; Ferraro, J. R.; Thorn, R. J.; Carlson, K. D.; Geiser, U.; Wang, H. H.; Kini, A. M.; Whangbo, M. H. *Organic Superconductors (Including Fullerenes)*; Prentice-Hall: Englewoods Cliffs, NJ, 1992.

(22) Katz, H. E. *J. Mater. Chem.* **1997**, *7*, 369.

relationships between the molecular structure, the propensity of cation radicals to dimerize, and the exact nature of the formed dimers. Elucidation of this latter point is certainly far from evident since besides evidences for  $\sigma$ -dimer formation in some cases,<sup>9</sup> there are also some examples of substrates capable to lead to either to  $\pi$ - or to  $\sigma$ -dimers depending on experimental conditions.<sup>24</sup>

On the other hand, since nTVs can be reversibly oxidized to a high charging rate (up to the hexa- and octacation),<sup>11,12</sup> the analysis of the possible dimerization of high radical state (tri- and pentacation radical) appears as particularly interesting. Such investigations are now underway and will be reported in future publications.

## Experimental Section

Compounds 1–6 were synthesized using previously reported procedures.<sup>11</sup> Cyclic voltammetry was performed in a three-electrode two-compartment cell equipped with a platinum microelectrode of  $7.85 \times 10^{-3} \text{ cm}^2$  area and a platinum wire counterelectrode. An Ag/AgCl electrode checked against the ferrocene/ferricinium couple ( $\text{Fc}^+/\text{Fc}$ ) before and after each experiment was used as reference. The electrolytic medium involved  $\text{CH}_2\text{Cl}_2$  (HPLC grade) and  $2 \times 10^{-1} \text{ mol L}^{-1}$  of tetrabutylammoniumhexafluorophosphate (TBAHP). All experiments were carried out in solutions preably deaerated by argon bubbling. Electrochemical experiments were carried out with a PAR 273 potentiostat with positive feedback compensation. For concentration dependent cyclic voltammetry the upper and lower limits of the initial concentration ( $1 \times 10^{-4} \text{ mol L}^{-1} < C_0 < 2 \times 10^{-3} \text{ mol L}^{-1}$ ) were defined by the maximum solubility of the unsubstituted compound 1 and by the detection of a still significant current at 293 K. ESR experiments have been run on a Bruker ESP 300 spectrometer driven with the Bruker ESP 1600 computer program. Experiments have been performed in the X-band frequency range with a TE102 cavity, at various temperatures between 300 and 150 K with a standard variable-temperature cryostat using cold nitrogen gas. The design of the ESR-electrochemical cell was inspired by the work of Fiedler et al.<sup>25</sup>

Time-resolved spectroelectrochemistry was performed using the previously described experimental setup.<sup>26</sup> UV–vis and near-IR experiments have been performed with Perkin-Elmer Lambda 19 near-IR spectrometer. Temperature-dependent optical spectra have been recorded with the aid of a Oxford cryostat using cold nitrogen gas.

JA990777W

(23) Kraft, A.; Grimsdale, A. C.; Holmes, A. B. *Angew. Chem., Int. Ed.* **1998**, *37*, 402.

(24) Yokoi, H.; Hatta, A.; Ishiguro, K.; Sawaki, Y., *J. Am. Chem. Soc.* **1998**, *120*, 12728, and references therein.

(25) Fiedler, D. A.; Koppenol, M.; Bond, A. M. *J. Electrochem. Soc.* **1995**, *142*, 862.

(26) Gaillard, F.; Levillain, E. *J. Electroanal. Chem.* **1995**, *410*, 133.